A polybasic motif in alternatively spliced KChIP2 isoforms prevents Ca^{2+} regulation of Kv4 channels

Received for publication, November 8, 2018, and in revised form, January 4, 2019 Published, Papers in Press, January 8, 2019, DOI 10.1074/jbc.RA118.006549

Jonathan G. Murphy[‡§1] **and Dax A. Hoffman**[§2]

From the [‡]*NIGMS and* [§]*Section on Molecular Neurophysiology, NICHD, National Institutes of Health, Bethesda, Maryland 20892*

Edited by Roger J. Colbran

The Kv4 family of A-type voltage-gated K^+ channels regulates the excitability in hippocampal pyramidal neuron dendrites and are key determinants of dendritic integration, spike timing-dependent plasticity, long-term potentiation, and learning. Kv4.2 channel expression is down-regulated following hippocampal seizures and in epilepsy, suggesting A-type currents as therapeutic targets. In addition to pore-forming Kv4 subunits, modulatory auxiliary subunits called K^+ channel–interacting proteins (KChIPs) modulate Kv4 expression and activity and are required to recapitulate native hippocampal A-type currents in heterologous expression systems. *KChIP* mRNAs contain multiple start sites and alternative exons that generate considerable N-terminal variation and functional diversity in shaping Kv4 currents. As members of the EF-hand domain–containing neuronal Ca^{2+} sensor protein family, KChIP auxiliary proteins may convey Ca^{2+} sensitivity upon Kv4 channels; however, to what degree intracellular Ca^{2+} regulates KChIP–Kv4.2 complexes is unclear. To answer this question, we expressed KChIP2 with Kv4.2 in HEK293T cells, and, with whole-cell patch–clamp electrophysiology, measured an ~1.5-fold increase in Kv4.2 current density in the presence of elevated intracellular Ca^{2+}. Intriguingly, the Ca^{2+} regulation of Kv4 current was specific to KChIP2b and KChIP2c splice isoforms that lack a putative polybasic domain that is present in longer KChIP2a1 and KChIP2a isoforms. Site-directed acidification of the basic residues within the polybasic motif of KChIP2a1 rescued Ca^{2+}-mediated regulation of Kv4 current density. These results support divergent Ca^{2+} regulation of Kv4 channels mediated by alternative splicing of KChIP2 isoforms. They suggest that distinct KChIP–Kv4 interactions may differentially control excitability and function of hippocampal dendrites.

The Kv4[3] family of voltage-gated K^+ channels is expressed across many brain regions where they perform a unique role. Tetrameric Kv4 channels mediate a fast activating and inactivating outward K^+ current in heterologous systems that produce the A-type current (I_A) in neurons (1). In area CA1 of the hippocampus, pyramidal neurons express primarily Kv4 channels in a graded manner that increases distal to the cell soma within the dendritic arbor (2). Within this cellular niche, Kv4 channels are key determinants of action potential repolarization, dendritic excitability and integration, spike timing-dependent plasticity, long-term potentiation, and learning (3–7). Down-regulation of Kv4 channel expression occurs following hippocampal seizures and in epilepsy suggesting A-type currents as targets for novel therapeutics (8, 9). Recapitulation of native hippocampal A-type K^+ currents in heterologous expression systems requires nonconducting modulatory auxiliary subunits known as K-channel interacting proteins (KChIPs) and dipeptidyl aminopeptidase-like proteins (DPPs) (10–12). Both KChIPs and DPPs work in concert to modify Kv4 expression and channel kinetics. In mammals, KChIPs are expressed from four genes in specific patterns throughout the brain that encode KChIPs 1–4 (13–15). In the hippocampus, KChIPs 2–4 predominate. The majority of KChIP isoforms promote forward trafficking to increase plasma membrane expression of Kv4 channels (16, 17). KChIPs also accelerate Kv4 channel opening, slow fast inactivation, shift voltage dependence of inactivation (VDI) toward more depolarized potentials, and accelerate recovery from inactivation (RFI) (13). Taken together, KChIPs regulate Kv4 channels to increase channel number and activity.

Responses to changing intracellular Ca^{2+} involves Ca^{2+}-sensing proteins that contain high-affinity Ca^{2+}-binding sites. As members of the neuronal Ca^{2+} sensor gene family, KChIPs contain Ca^{2+}-binding EF hands, two each in N- and C-terminal lobules (13). Only the two C-terminal EF hands (EF-3 and EF-4) are thought to bind Ca^{2+} under normal conditions, whereas the N-terminal EF-hands are degenerated such that EF-1 does not bind Ca^{2+} and EF-2 binds Mg^{2+} preferentially over Ca^{2+} (18–22). The EF-hands of KChIP family members are highly conserved suggesting that Ca^{2+} binding is important for KChIP function. Indeed, *in vitro* withdrawal of Ca^{2+} from KChIP

This work was supported by National Institutes of Health Intramural Funds FI2 GM120004 from NIGMS (to J. G. M.) and Z01 HD008755 from NICHD (to D. A. H.). The authors declare that they have no conflicts of interest with the contents of this article. The content is solely the responsibility of the authors and does not necessarily represent the official views of the National Institutes of Health.

This article contains Fig. S1.

[1] To whom correspondence may be addressed: Rm. 3C-908, Bldg. 35, 35 Lincoln Dr., NIGMS, National Institutes of Health, Bethesda, MD 20892. Tel.: 301-451-4542; E-mail: jonathan.murphy@nih.gov.

[2] To whom correspondence may be addressed: Rm. 3C-905, Bldg. 35, 35 Lincoln Dr., Section on Molecular Neurophysiology, NICHD, National Institutes of Health, Bethesda, MD 20892. Tel.: 301-402-6772; Fax: 301-402-4777; E-mail: hoffmand@mail.nih.gov.

[3] The abbreviations used are: Kv4, voltage-gated K^+ channel 4; KChIP, K^+ channel interacting protein; DPP, dipeptidyl peptidase-like protein; VDI, voltage dependence of inactivation; RFI, recovery from inactivation; HEDTA, *N*-(2-hydroxyethyl)ethylenediamine-*N*,*N*′,*N*′-triacetic acid; MEM, minimal essential medium; DMEM, Dulbecco's modified Eagle's medium; CaM, calmodulin; CaN, calcineurin; ER, endoplasmic reticulum; VDA, voltage dependence of activation; ANOVA, analysis of variance.

results in conformational changes, including reduced rigidity and loss of helical content (20, 21, 23). Understanding the contribution of Ca^{2+} to KChIP regulation of Kv4 complexes is of great interest because it suggests the potential for feedback regulation in neurons. Many studies have made mutations to the EF-hands of KChIP family members to tease apart relative functions for EF-2, EF-3, and EF-4 in Kv4 regulation (13, 24). Although this approach is informative, Ca^{2+} binding and intrinsic structural roles for the EF-hands cannot be dissociated. However, published studies examining the role of intracellular Ca^{2+} in regulation of KChIP–Kv4.2 complexes have been performed in several different cell types, using various KChIP/Kv4 family members and differing methods for elevating or reducing intracellular Ca^{2+}. Thus, there are inconsistencies in the literature regarding Ca^{2+}-KChIP regulation of Kv4 function. Differing reports have shown Ca^{2+} may either retain or disrupt KChIP-Kv binding, increase or decrease channel currents, or alter channel gating in various ways (13, 24–27).

Kv4.2 and Kv4.3 are the most abundant Kv4 subunits expressed in excitable tissues, including the heart and brain. In area CA1 of the hippocampus Kv4.2 predominates and is responsible for the A-type current in pyramidal neuron dendrites. Significant functional diversity in A-type currents may arise through the multiple 5′ start sites and alternative N-terminal exons in the four *Kcnip* genes that generates 17 different proteins with diverse tissue-specific expression patterns (14, 15). *In situ* hybridization localization of KChIPs 1–4 suggest that KChIP2 and KChIP4 are the most abundant KChIPs in area CA1 of the hippocampus (14). RT-PCR analysis of whole-hippocampus extracts suggests that KChIP2a and KChIP4a predominate, whereas KChIP2b and -2c are present to a lesser extent (14, 28). In the future, more sensitive measurements of KChIP splice isoform expression are needed to determine how spatial differences may lead to region and cell-type specificity of Kv4 regulation.

Although much research has focused on the role of the EF-hands in binding Ca^{2+}, the influence of the variable N-terminal regions on Ca^{2+} regulation remains unclear. In this study, we show that elevated intracellular Ca^{2+} regulates Kv4 function by increasing current density. Ca^{2+} regulation is conserved across the Kv4 family but is specific to short isoforms of KChIP2 and to KChIP3a. A shared basic and hydrophobic N-terminal domain in KChIP2a1 and KChIP2a confers resistance to Kv4 regulation by intracellular Ca^{2+}.

Results

KChIP2c regulates Kv4.2 channel kinetics and inactivation

KChIPs 1–4 are all assumed to bind Ca^{2+} under normal circumstances; however, KChIP2c has previously been reported to bind to Kv4.2 in a Ca^{2+}-dependent manner (25). We first determined whether KChIP2c maintained regulation of Kv4.2 channels in nominal Ca^{2+} (0 Ca^{2+}, 10 mM EGTA). To assess KChIP2c regulation of Kv4.2 currents, we expressed Kv4.2 alone (Fig. 1*a*) or in the presence of KChIP2c (Fig. 1*b*) in HEK293T cells and performed whole-cell patch–clamp electrophysiology (Fig. 1*c*). KChIP2c regulation of Kv4.2 peak currents were measured using a voltage-clamp protocol. Because Kv4 channels inactivate at relatively hyperpolarized holding potentials (−70.24 ± 0.91 mV; Table 1), a pre-pulse to −120 mV is used to alleviate latent inactivation. A step to +60 mV elicits an outward K^+ current carried by Kv4.2 channels (Fig. 1*d*). As predicted from the established literature (25), coexpression of KChIP2c increased Kv4.2 current density ~2.07-fold (Fig. 1*e*) and accelerated the 10–90% current rise time ~1.53-fold (Fig. 1*f*). When fit to a double exponential (Fig. S1), KChip2c coexpression slowed the fast rate of inactivation ~3-fold (Fig. 1*g*) but had no effect on the second, slower component of decay (Fig. 1*h*). After stepping through a series of increasing voltages, we found that KChIP2c coexpression had no effect on the voltage dependence of activation (VDA) for Kv4.2; however, KChIP2c shifted the VDI to more depolarized potentials as described previously for most KChIP family members (Fig. 1*i*; Table 1) (15). KChIP2c coexpression also dramatically accelerated the RFI as shown by others (Fig. 1*j*; Table 1) (25). Based on these results, we can confirm that at low-intracellular free Ca^{2+} (0 Ca^{2+}/10 mM EGTA), KChIP2c regulation of Kv4 current is intact.

Ca^{2+} regulation of Kv4.2 current density requires KChIP2c

To assess the Ca^{2+} dependence of Kv4.2 function, whole-cell patch–clamp recordings were performed in either nominal Ca^{2+} (0 Ca^{2+} and 10 mM EGTA) or ~10 μM Ca^{2+} (5 mM Ca^{2+}/10 mM hydroxyethyl)ethylenediamine-*N*,*N*′,*N*′-triacetic acid (HEDTA)) (Fig. 2, *a* and *b*). Although the high affinity Ca^{2+} chelator EGTA is ideal for maintaining low levels of intracellular Ca^{2+}, even small pipetting errors can lead to large differences in free Ca^{2+} above 1 μM. Intracellular free Ca^{2+} is better clamped within the 10 μM range using the low-affinity Ca^{2+} buffer HEDTA (29). In cells expressing Kv4.2 alone, 10 μM Ca^{2+} affected neither K^+ current density, VDA, VDI, or RFI (Fig. 2*c*; Table 2). To assess whether Ca^{2+} regulates Kv4.2 channels through KChIP auxiliary proteins we coexpressed KChIP2c. Coexpression of KChIP2c enhanced K^+ current density under nominal Ca^{2+} as described above (Fig. 1*e*, and Fig. 2*d*; Table 1); however, in the presence of KChIP2c and ~10 μM Ca^{2+}, K^+ current density was increased, whereas VDA, VDI, and RFI were not affected (Fig. 2*d*; Table 1). To determine whether the Ca^{2+} regulated increase in current density was evident in the presence of another obligatory Kv4 subunit DPP6, we measured the same electrophysiological parameters in cells coexpressing Kv4.2, KChIP2c, and DPP6 (Fig. 2*e*). Although the trend for a Ca^{2+}-regulated increase in peak current density remained, it did not achieve statistical significance (Fig. 2*e*; Table 2). The effect of Ca^{2+} was most pronounced on Kv4.2–KChIP2c K^+ currents elicited at the peak of the G-V curve. To more closely examine the effects of Ca^{2+} on peak currents, we analyzed both the magnitude and kinetics of Kv4.2 currents evoked with a single voltage step to +60 mV in HEK293T cells expressing Kv4.2 and KChIP2c (Fig. 3*a*). As observed previously, peak K^+ currents were larger in magnitude in the presence of 10 μM Ca^{2+} (Fig. 3, *a* and *b*). Additionally, Ca^{2+} accelerated the 10–90% rise time and the fast τ_1 of current decay while leaving the second, slower τ_2 component unchanged (Fig. 3, *c*–*e*). However, Ca^{2+} regulation of 10–90% rise time also occurred in the absence of KChIP2c suggesting this is a KChIP-independent effect (Table 2). Taken together,

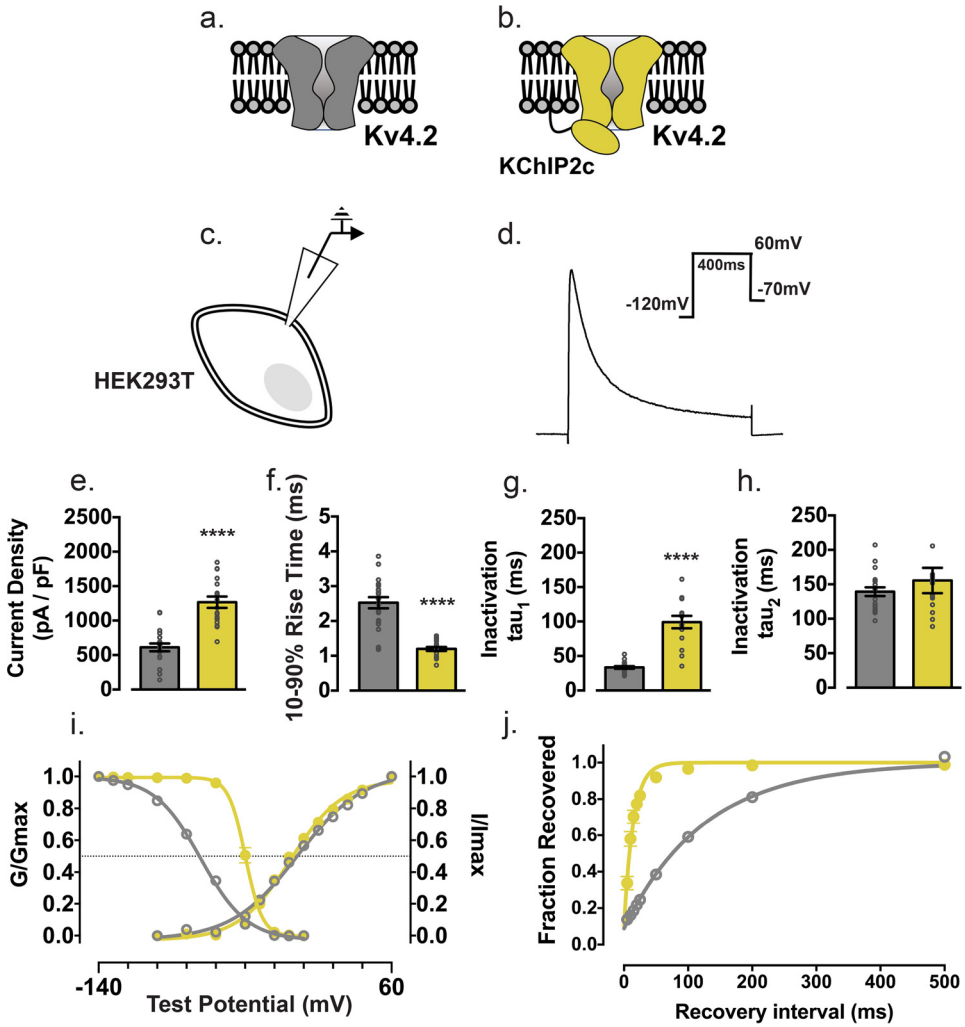

Figure 1. KChIP2c regulates Kv4.2 channel current density and kinetics. *a* and *b,* experimental configuration in which Kv4.2 is expressed alone (*gray*) or coexpressed with KChIP2c (*yellow*). This color scheme is used throughout Fig. 1. *c,* voltage-clamp recording configuration for measuring Kv4.2 K^+ currents. *d,* representative peak outward K^+ current mediated by Kv4.2 and evoked with a step depolarization. *e,* peak outward K^+ current density. Raw current was normalized to cell size measured by whole-cell capacitance on cell break-in. *f,* time required for the outward K^+ current to rise from 10 to 90% of the peak. *g* and *h,* kinetics of channel inactivation was measured by fitting the falling phase of peak outward K^+ current with a double-exponential decay and comparing fast (*g*) or slow (*h*) components across conditions. *i,* normalized conductance and current *versus* applied test membrane potential for VDA and VDI protocols. *Colored connecting lines* represent Boltzman curve fits. *j,* time-dependent fractional recovery of peak outward K^+ current after a VDI prepulse. Curves are fitted to a single exponential function. *Error bars* represent mean ± S.E. *, $p < 0.05$; ****, $p < 0.0001$ by unpaired *t* test. Refer to Tables 1 and 2 for numerical data and replicate information.

elevated intracellular Ca^{2+} regulates Kv4.2 current density and requires the presence of KChIP2c.

Ca^{2+} regulation is conserved across the Kv4 family of K^+ channels

Although Kv4.2 is the predominant Kv4 isoform in CA1 neurons of the hippocampus, Kv4.1 and Kv4.3 transcripts and proteins are also present, albeit at significantly lower levels (12, 30–32). Kv4.1 is expressed at relatively low levels throughout the brain, whereas Kv4.3 is more abundantly expressed in dentate gyrus, hippocampal interneurons, cerebellum, and cardiac tissues. Kv4.1, Kv4.2, and Kv4.3 share >62% sequence conservation in domains involved in binding to KChIPs and are functionally regulated by KChIP isoforms (Fig. 4*a*) (13, 33). To determine whether Ca^{2+} regulation through KChIP2c is conserved across the Kv4 family, we coexpressed either Kv4.1, Kv4.2, or Kv4.3 with KChIP2c in HEK293T cells and recorded voltage-gated K^+ currents. Under nominal Ca^{2+} conditions, KChIP2c regulated Kv4.1 and Kv4.3 currents similarly to Kv4.2 by shifting VDI to more depolarized potentials and accelerating RFI (Table 1). KChIP2c also increased peak K^+ current density, accelerated rise time, and slowed the fast τ_1 component of current decay. Unlike Kv4.2, the VDA of both Kv4.1 and Kv4.3 underwent a small shift toward more depolarized potentials. In the presence of ~10 μM Ca^{2+}, Kv4.1–4.3 VDA, VDI, and RFI were unchanged (Fig. 4*b*); however, Ca^{2+} increased Kv4.1 and Kv4.3 current density ~1.5-fold, a level similar to what was observed for Kv4.2 (Fig. 4*c*). Unlike Kv4.2, the 10–90% rise time of Kv4.1 or Kv4.3 was unchanged in the presence of ~10 μM Ca^{2+} (Fig. 4, *d–f*). These results suggest that Ca^{2+} increases K^+ current density across the Kv4 channel family in a KChIP2c-dependent manner.

A polybasic domain in KChIP2 isoforms prevents Ca^{2+} regulation of KChIP–Kv4 complexes

The *Kcnip1–4* genes contain multiple alternatively spliced 5′ exons that generate considerable N-terminal variation and

Table 1

Biophysical properties of Kv4 family members in nominal 0 μM free Ca^{2+} (gray boxes) or ~10 μM free Ca^{2+} (red boxes)

I_K indicates peak voltage-gated K^+ current. All entries describe the mean ± S.D.

Condition	$V_{1/2}$ VDA (mV)	$V_{1/2}$ VDI (mV)	Tau of RFI (ms)	I_K Density (pA/pF)	I_K 10-90% Rise (ms)	I_K Tau_1 (ms)	I_K Tau_2 (ms)
Kv4.1 only	-10.38 +/- 2.40 n = 8	-65.40 +/- 2.34 n = 7	90.81 +/- 12.72 n = 7	537.8 +/- 244.95 n = 6	1.71 +/- 0.22 n = 6	24.7 +/- 5.37 n = 6	165.4 +/- 14.97 n = 6
Kv4.1 KChip2c	-0.00 +/- 1.15* n = 17	-43.48 +/- 1.68* n = 16	27.19 +/- 7.32* n = 15	739.1 +/- 340.2 n = 11	1.45 +/- 0.55 n = 14	46.13 +/- 21.30 n = 14	111.3 +/- 37.17* n = 9
Kv4.1 KChip2c + 10 μM Ca^{2+}	-2.25 +/- 1.28*# n = 21	-44.77 +/- 1.88* n = 20	21.28 +/- 4.03* n = 18	1173 +/- 458.1*# n = 13	1.40 +/- 0.46 n = 18	45.16 +/- 30.75 n = 19	100.5 +/- 39.95* n = 19
Kv4.2 only	-4.23 +/- 3.44 n = 18	-70.24 +/- 3.76 n = 17	125.3 +/- 25.65 n = 17	611.5 +/- 252.32 n = 20	2.53 +/- 0.72 n = 20	33.35 +/- 8.21 n = 20	139.3 +/- 28.26 n = 20
Kv4.2 KChIP2c	-6.81 +/- 1.80* n = 16	-39.76 +/- 1.65* n = 17	14.45 +/- 4.45* n = 14	1267 +/- 340.3* n = 17	1.20 +/- 0.25* n = 17	99.19 +/- 34.59* n = 15	138.9 +/- 30.27 n = 14
Kv4.2 KChIP2c + 10 μM Ca^{2+}	-5.00 +/- 1.39* n = 15	-39.68 +/- 1.92* n = 16	14.76 +/- 4.52* n = 10	1643 +/- 422.4*# n = 18	1.054 +/- 0.17* n = 18	65.89 +/- 19.77*# n = 18	124.0 +/- 39.87 n = 17
Kv4.3 only	-7.64 +/- 2.46 n = 10	-51.47 +/- 4.53 n = 8	119.0 +/- 26.22 n = 8	768 +/- 767.92 n = 8	1.95 +/- 0.42 n = 8	41.66 +/- 25.76 n = 7	125.2 +/- 43.10 n = 7
Kv4.3 KChIP2c	-3.69 +/- 2.75* n = 19	-35.78 +/- 2.35* n = 19	27.19 +/- 7.32* n = 15	938.2 +/- 612.3 n = 17	1.39 +/- 0.41* n = 17	68.98 +/- 81.56 n = 16	136.1 +/- 43.08 n = 16
Kv4.3 KChIP2c + 10 μM Ca^{2+}	-3.90 +/- 2.56* n = 15	-37.42 +/- 1.42* n = 15	25.77 +/- 5.23* n = 13	949 +/- 819.9 n = 15	1.28 +/- 0.27* n = 15	40.30 +/- 34.7 n = 15	149.6 +/- 52.79 n = 15

* and # represent statistical significance ($0.05 > p > 0.0001$) by one-way ANOVA and Tukey's post-test (Kv4, 0 μM Ca^{2+} *versus* Kv4, KChIP, 0 μM Ca^{2+}, or Kv4, KChIP, 10 μM Ca^{2+} (*); Kv4, KChIP, 0 μM Ca^{2+} *versus* Kv4; KChIP, 10 μM Ca^{2+} (#).

functional diversity (Fig. 5*a*) (14, 15). To determine whether Ca^{2+} regulation is conserved across all isoforms of the KChIP2 family, we coexpressed either KChIP2a1, KChIP2a, KChIP2b, or KChIP2c with Kv4.2 and measured peak voltage-gated K^+ currents. In the presence of ~10 μM Ca^{2+}, KChIP2b expression resulted in an increase in Kv4.2 K^+ current density to a similar extent as KChIP2c (Fig. 5*b*), whereas rise time and inactivation kinetics of Kv4.2 were not affected (Table 2). We also tested a select number of KChIP isoforms from the KChIP1, -3, and -4 gene families and found that only KChIP3a–Kv4.2 complexes responded to elevated Ca^{2+} with increased current density equal in magnitude to the short forms of KChIP2 (Tables 2 and 3). Surprisingly, the longer KChIP2 isoforms, KChIP2a1 and KChIP2a, did not respond to ~10 μM Ca^{2+} (Fig. 5*b*; Table 2). Sequence alignment of KChIP2 isoforms identified a 16-amino acid sequence unique to Ca^{2+}-insensitive KChIP isoforms that consisted of basic residues flanked by hydrophobic and aliphatic amino acids that resembled a polybasic motif (Fig. 5*c*). To determine whether the putative polybasic motif present in KChIP2a1 and KChIP2a was required for KChIP resistance to Ca^{2+} regulation, we acidified this stretch by mutating R*X*HR*X*R to D*X*DD*X*D. Whole-cell voltage– clamp recordings of Kv4.2 currents revealed an ~1.5-fold increase in peak current density of KChIP2a1DDDD-Kv4 expressing cells in the presence of ~10 μM intracellular Ca^{2+} (Fig. 5*d*). These results support an inhibitory role for the putative polybasic motif present in longer KChIP2a1 and KChIP2a isoforms. This motif limits sensitivity of Kv4 complexes to regulation by elevated intracellular Ca^{2+}.

Discussion

Here, we provide evidence for a subset of KChIP isoforms that enhance Kv4-type voltage-gated K^+ channel current density in

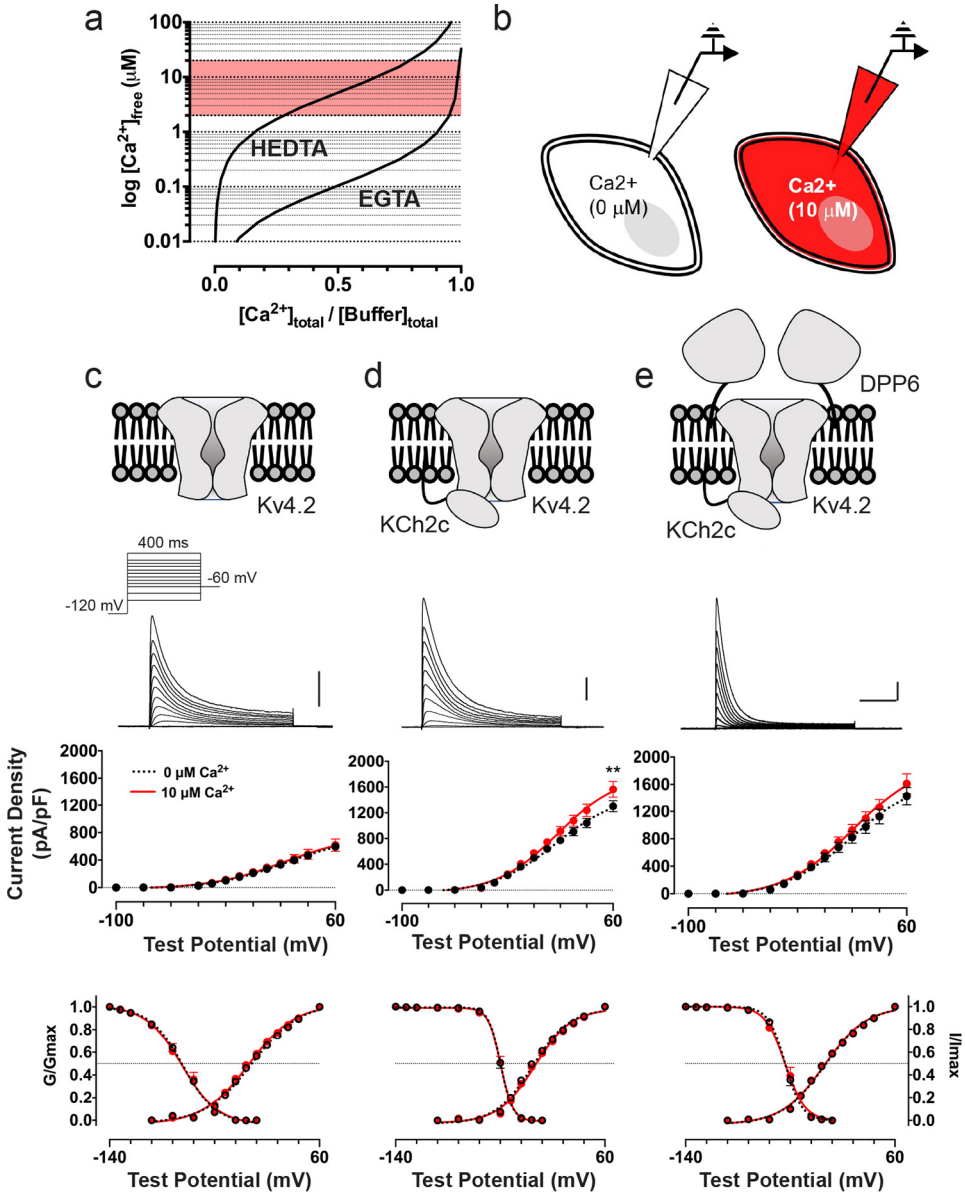

Figure 2. Intracellular Ca^{2+} regulates Kv4.2 channel current density. *a,* theoretical free intracellular Ca^{2+} concentration at varying ratios of Ca^{2+} and buffer. Free Ca^{2+} was calculated using webmaxchelator (https://web.stanford.edu/~cpatton/webmaxcS.htm) (Please note that the JBC is not responsible for the long-term archiving and maintenance of this site or any other third party hosted site.). *b,* schematic describing intracellular dialysis of buffering solutions to clamp free Ca^{2+}. Color scheme is used throughout Figs. 2–5 for nominal 0 μM free Ca^{2+} (*black/white*) and ~10 μM free Ca^{2+} (*red*). *c–e,* construct expression (*top*), VDA protocol (*above-middle inset*), representative VDA K^+ currents (*above-middle*), VDA current density *versus* test potential (*below-middle*), and normalized conductance and current *versus* applied test membrane potential for VDA and VDI protocols (*bottom,* Kv4.2 data also appears in Fig. 4*b*). Curves were fitted to a Boltzmann function. *Horizontal scale bar,* 100 ms; *vertical scale bars,* 1 nA. *Error bars* represent mean ± S.E. **, $p < 0.01$ by unpaired *t* test. Refer to Tables 1 and 2 for numerical data and replicate information.

response to elevations in intracellular Ca^{2+}. KChIPs that transmit changes in intracellular Ca^{2+} to Kv4 channels and those that do not share highly conserved EF-hand domains within the globular protein core; however, unique N-terminal domains generated by alternatively spliced exons differentiate Ca^{2+}-regulated KChIPs from Ca^{2+}-insensitive KChIP isoforms. Using whole-cell voltage–clamp recordings in HEK293T cells expressing Kv4 channels and an array of KChIP isoforms, we show that elevated intracellular Ca^{2+} has no effect on KChIP2a1 and KChIP2a. Conversely, cells expressing KChIP2b, KChIP2c, and KChIP3a show ~1.5-fold increase in Kv4 K^+ current density. We have identified a novel motif shared by KChIP2a1 and KChIP2a that is absent from the Ca^{2+}-sensitive KChIP2b, KChIP2c, and KChIP3a isoforms. Comparisons of the variable N-terminal domains suggest that a conserved amino acid sequence containing basic amino acids limits Ca^{2+} sensitivity of KChIP2a1 and KChIP2a. Acidification of the KChIP2a1 basic motif confers Ca^{2+} sensitivity, increasing Kv4.2 current density in a Ca^{2+}-dependent manner. Taken together, these data support a role for Ca^{2+} regulation of Kv4 channel current density in neuronal populations that express a subset of KChIP isoforms.

Ca^{2+} sensing by KChIPs

In published studies of the Ca^{2+}-dependent/independent regulation of Kv4 by KChIPs, many groups have used a series of KChIP EF-hand mutants (EFmut) to inhibit Ca^{2+} binding.

Table 2

Comparison of biophysical properties between Kv4.2-KChIP2 isoform complexes in nominal 0 μM free Ca^{2+} (gray) or 10 μM free Ca^{2+} (red)

I_K indicates peak voltage-gated K^+ current. All entries describe the mean ± S.D.

Condition	$V_{1/2}$ VDA (mV)	$V_{1/2}$ VDI (mV)	Tau of RFI (ms)	I_K Density (pA/pF)	I_K 10-90% Rise (ms)	I_K Tau_1 (ms)	I_K Tau_2 (ms)
Kv4.2 only	-4.23 +/- 3.44 n = 18	-70.24 +/- 3.76 n = 17	125.3 +/- 25.65 n = 17	611.5 +/- 252.32 n = 20	2.53 +/- 0.72 n = 20	33.35 +/- 8.21 n = 20	139.3 +/- 28.26 n = 20
+ 10 μM Ca^{2+}	-7.39 +/- 4.34* n = 14	-71.05 +/- 6.96 n =12	111.6 +/- 20.33 n = 11	752.0 +/- 410.94 n = 18	1.89 +/- 0.51* n = 18	29.04 +/- 8.27 n = 18	126.6 +/- 33.35 n = 18
Kv4.2 KChIP2a1	-7.79 +/- 1.53 n = 9	-53.88 +/- 1.68 n = 9	12.98 +/- 3.03 n = 8	1082 +/- 247.09 n = 8	1.25 +/- 0.34 n = 8	76.84 +/- 13.83 n = 8	127.9 +/- 17.82 n = 8
+ 10 μM Ca^{2+}	-4.79 +/- 1.20* n = 9	-55.48 +/- 1.02 n = 9	13.71 +/- 2.33 n = 7	960.0 +/- 401.6 n = 10	1.07 +/- 0.28 n = 10	67.28 +/- 17.08 n = 10	117.5 +/- 27.45 n = 10
Kv4.2 KChIP2a	-5.35 +/- 1.28 n = 12	-51.21 +/- 1.59 n = 12	12.94 +/- 2.49 n = 11	1471 +/- 551.48 n = 12	1.31 +/- 0.66 n = 12	81.37 +/- 30.55 n = 12	120.8 +/- 45.00 n = 12
+ 10 μM Ca^{2+}	-3.19 +/- 1.37* n = 13	-50.76 +/- 1.21 n = 12	15.21 +/- 3.18 n = 9	1444 +/- 385.06 n = 11	1.33 +/- 0.40 n = 11	59.30 +/- 16.55* n = 11	113.6 +/- 22.16 n = 11
Kv4.2 KChIP2b	-2.96 +/- 1.36 n = 10	-51.40 +/- 1.80 n = 10	15.23 +/- 2.91 n = 9	957.6 +/- 315.75 n = 10	1.12 +/- 0.19 n = 10	63.38 +/- 19.70 n = 10	104.5 +/- 18.11 n = 10
+ 10 μM Ca^{2+}	-2.19 +/- 1.16 n = 11	-50.28 +/- 2.19 n = 11	13.44 +/- 3.23 n = 7	1489 +/- 280.6* n = 10	1.03 +/- 0.18 n = 9	64.69 +/- 10.98 n = 9	95.65 +/- 18.12 n = 9
Kv4.2 KChIP2c	-6.81 +/- 1.80 n = 16	-39.76 +/- 1.65 n = 17	14.45 +/- 4.45 n = 14	1267 +/- 340.3 n = 17	1.20 +/- 0.25 n = 17	99.19 +/- 34.59 n = 15	138.9 +/- 30.27 n = 14
+ 10 μM Ca^{2+}	-5.00 +/- 1.39* n = 15	-39.68 +/- 1.92 n = 16	14.76 +/- 4.52 n = 10	1643 +/- 422.4* n = 18	1.054 +/- 0.17* n = 18	65.89 +/- 19.77* n = 18	124.0 +/- 39.87 n = 17
Kv4.2 KChIP2c DPP6	-6.96 +/- 4.71 n = 12	-44.93 +/- 2.04 n = 12	14.66 +/- 8.09 n = 11	1447 +/- 433.0 n = 12	0.656 +/- 0.17 n = 12	45.62 +/- 8.99 n = 11	82.33 +/- 50.54 n = 10
+ 10 μM Ca^{2+}	-7.55 +/- 4.57 n = 12	-44.95 +/- 3.57 n = 12	18.67 +/- 16.42 n = 11	1603 +/- 457.6 n = 12	0.598 +/- 0.10 n = 12	41.04 +/- 17.64 n = 11	73.49 +/- 29.72 n = 11

* represents statistical significance ($0.05 > p > 0.0001$) by unpaired *t* test. All comparisons are made within each plasmid expression condition between 0 μM free Ca^{2+} and 10 μM free Ca^{2+}.

In these experiments, an Asp to Ala mutation is made at position 1 of one or more KChIP EF-hands. EFmut KChIPs are then coexpressed with Kv4 channels, and the Ca^{2+}-dependent effects of KChIP regulation on Kv4 currents are inferred. Each successive EF-hand mutation leads to a progressive loss of KChIP regulation of Kv4 channels with a particular requirement for EF-3 and EF-4, the EF-hands known to bind Ca^{2+} with highest affinity (18–24, 34). However, mutations to EF-hand domains disrupt tertiary structure, potentially leading to misinterpretation of results that may arise independent of Ca^{2+} binding (35). It has also been reported that EFmut KChIP1 is misfolded, further suggesting that EF-hand mutations affect KChIP structure (23). With these caveats in hand, some reports have shown that EFmut KChIPs retain Kv4.2 binding suggesting a Ca^{2+}-independent KChIP–Kv4 interaction (13, 25). Other groups using similar methodologies found that KChIP–Kv4 binding is Ca^{2+}-dependent (26, 27). In the work presented here, without disrupting KChIP EF-hands, we show that KChIP and Kv4 channels remain associated after dialysis with 0 Ca^{2+}, 10 mM EGTA intracellular solution, a low Ca^{2+} condition that disrupts KChIP helical structure *in vitro* (23).

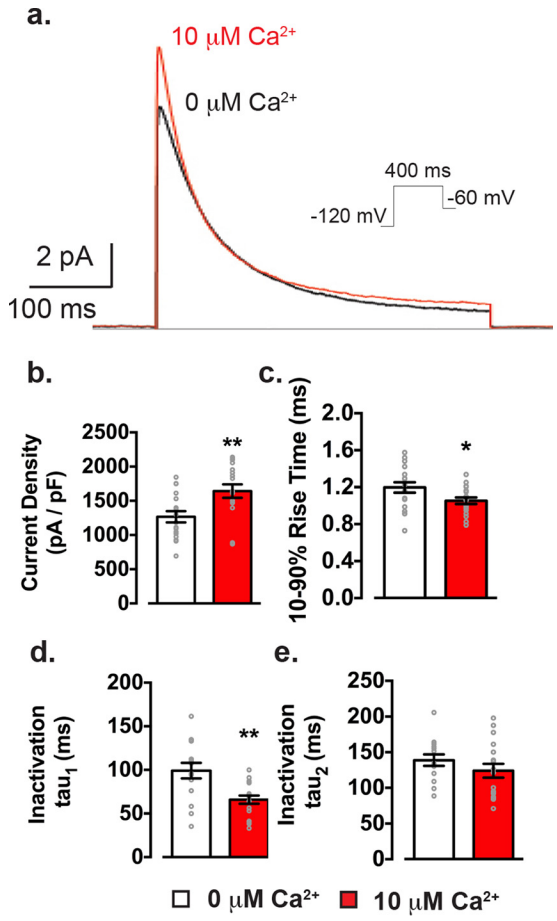

Figure 3. Intracellular Ca^{2+} regulates Kv4.2 peak current. *a,* representative evoked outward K^+ current in HEK293T cells expressing Kv4.2 and KChIP2c either in nominal 0 μM Ca^{2+} (*black trace*) or ~10 μM free Ca^{2+} (*red trace*). *b,* peak outward K^+ current density. Raw current was normalized to cell size measured by whole-cell capacitance on cell break-in. *c,* time required for the outward K^+ current to rise from 10 to 90% of the peak. *d* and *e,* kinetics of channel inactivation was measured by fitting the falling phase of peak outward K^+ current with a double-exponential decay and comparing fast (*d*) or slow (*e*) components across conditions. *Error bars,* mean ± S.E. *, $p < 0.05$; **, $p < 0.01$ by unpaired *t* test. Refer to Table 2 for numerical data and replicate information.

KChIP regulation of Kv4 channel kinetics, VDI, and RFI remains intact for tens of minutes after attaining the whole-cell patch–clamp configuration suggesting low Ca^{2+} does not disrupt the KChIP–Kv4 interaction. This suggests that either EGTA cannot chelate Ca^{2+} already coordinated within the KChIP–Kv4 structure, does not outcompete the KChIP EF hands for Ca^{2+}, or Ca^{2+} is not required for KChIP–Kv4 complex formation, as has been put forward by Groen and Bahring (36). Along those lines, studies have suggested that the KChIP–Kv4 complex is co-assembled and traffics together from the ER or the Golgi (16, 37, 38). Importantly, KChIPs do not regulate unitary Kv4 conductance suggesting changes in single channel conductance states is an unlikely mechanism for Ca^{2+} regulation of Kv4 currents (39). Instead, increased current density is likely due to an increase in KChIP–Kv4 protein expression and plasma membrane surface trafficking (13, 16, 25, 38, 39). Therefore, our results suggest a post-ER/Golgi pool of Kv4 may be recruited to the plasma membrane by Ca^{2+} in a KChIP-dependent manner (Fig. 6).

Ca^{2+} regulation of KChIP–Kv4 plasma membrane localization

KChIPs, like other members of the neuronal Ca^{2+} sensor-1 family, are composed of N- and C-terminal lobules each containing two EF hands. Although the globular structures of KChIP1, KChIP3, and KChIP4 have been described (40–42), only the N-terminal domain of KChIP4a has been captured suggesting most KChIPs have an unstructured and flexible N-terminal domain *in vitro*. Two separate groups have independently described identical structures for the channel complex containing KChIP1 and Kv4.3 (23, 43). These KChIP1–Kv4.3 structures are likely similar to those occurring between the various KChIP–Kv4 combinations examined above; however, without crystallized KChIP N termini, the published KChIP1–Kv4.3 structure can only be generalized to globular KChIP–Kv4 interactions. When bound to Kv4.3, KChIP1 sequesters the cytoplasmic N terminus of Kv4.3 within a deep hydrophobic pocket. KChIP sequestration is thought to be responsible for slowing of Kv4 N-type inactivation (44). Although the EF-hand–containing globular core is highly conserved, the four mammalian *Kcnip* genes have multiple transcription start sites and alternative 5′ exons that result in at least 17 isoforms with differing N-terminal domains (15). The variable N-terminal regions differentially regulate Kv4 channel properties, subcellular localization to lipid membranes, and Ca^{2+} sensitivity, as described here. KChIP1a, KChIP1b, and KChIP4a are all considered membrane-associated either through *N*-myristoylation (KChIP1a/KChIP1b) or due to a transmembrane α-helix (KChIP4a) (45). These KChIP–Kv4 complexes do not respond to Ca^{2+} suggesting Ca^{2+} resistance may be mediated through membrane localization. KChIP2c is considered cytoplasmic, whereas KChIP2a1, KChIP2a, KChIP2b, and KChIP3a contain putative palmitoylation sites and may associate with the plasma membrane in a regulated manner dependent upon palmitoyltransferase activity. KChIP2c and KChIP3a have a primarily cytoplasmic localization when compared with KChIP2a and KChIP2b. However, upon coexpression with Kv4.3, each KChIP is effectively recruited to the plasma membrane to regulate Kv4.3 channels similarly (28). Additionally, differential regulation by KChIP isoforms may influence Kv4 surface stability, channel-recycling rate, or ratio of surface and intracellular complexes. In one study, KChIP3a was shown to bind to recycling endosome-related proteins (Rabs) in a Ca^{2+}-independent manner (46). This study also identified the KChIP3a N terminus as a Ca^{2+}-dependent binding site for calmodulin (CaM) and a Ca^{2+}-independent binding site for the phosphatase calcineurin (CaN). The presence of KChIP3a was shown to increase the catalytic activity of CaM–CaN *in vitro*. Intriguingly, CaN is known to promote Kv4.2 surface expression in hippocampal neurons (47, 48); this represents one trafficking mechanism that may explain the Ca^{2+} dependence of membrane insertion, at least for the KChIP3a isoform. KChIP2 N-terminal regions have a notable conservation of hydrophobic and basic amino acids (66% of amino acids in KChIP2a). Such sequences resemble putative polybasic motifs. Polybasic motifs promote association with the plasma membrane through electrostatic interactions with phospholipid headgroups. An alternatively spliced polybasic motif in large conductance Ca^{2+}- and

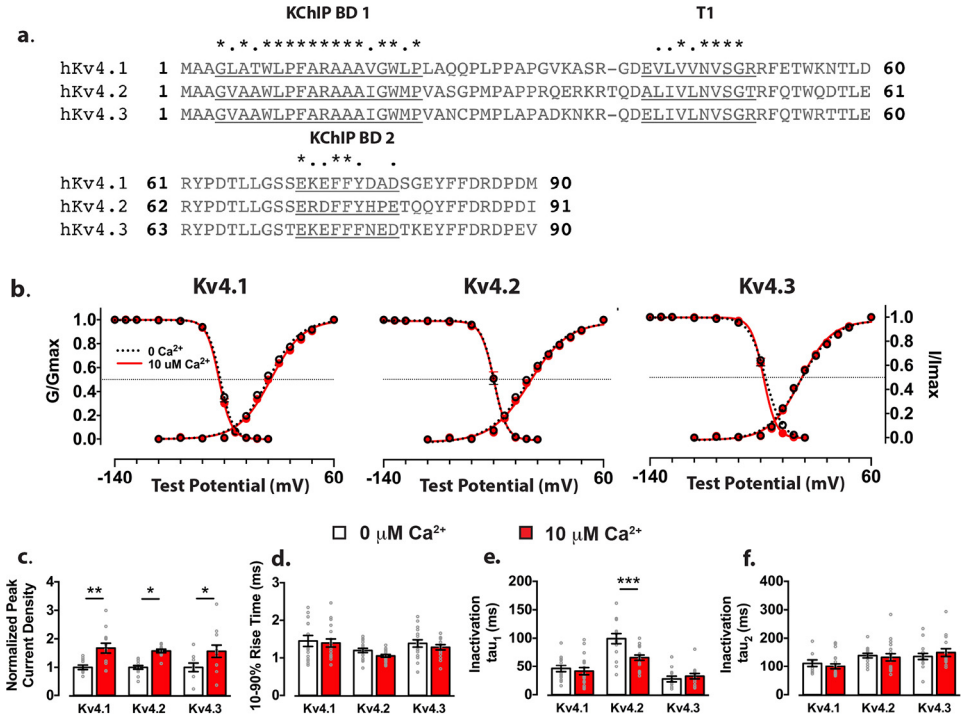

Figure 4. Ca^{2+} regulation is conserved across the Kv4 family. *a,* sequence alignment of the intracellular N-terminal domains of Kv4 family members. Proposed KChIP-binding domains (*KChIP BD 1/2*) and the Kv4 tetramerization domain (*T1*) are shown. *b,* normalized conductance and current *versus* applied test membrane potential for VDA and VDI protocols in Kv4.1, Kv4.2 (data also appears in Fig. 2*d*), or Kv4.3 and KChIP2c expressing HEK293T cells are shown. *c,* because of day-to-day variability of Kv4.1 and Kv4.3 construct expression, current density (pA/picofarad (pF)) was normalized by day of experiment. Statistical analysis by two-way ANOVA showed a significant effect of treatment ($p < 0.0001$) but not by Kv4 isoform expression (due to normalization) or the interaction ($p = 0.9076$). Sidak's multiple comparisons among the Kv4 isoforms in control and treated conditions yielded significant differences within groups (Kv4.1, $p = 0.0026$; Kv4.2, $p = 0.0107$; and Kv4.3, $p = 0.0253$). *d* and *e,* macroscopic channel kinetics are presented as described in Fig. 3. *d,* statistical analysis of 10–90% rise times found significant differences among Kv4 isoforms ($p = 0.0041$) but not by treatment ($p = 0.1735$) or the interaction ($p = 0.8888$). Comparison of control and 10 μM Ca^{2+} 10–90% rise time within Kv4 isoforms revealed no differences (Kv4.1, $p = 0.9626$; Kv4.2, $p = 0.5717$; and Kv4.3, $p = 0.8137$). *e,* significant differences in the variation between treatment ($p = 0.0320$), Kv4 isoform expression ($p < 0.0001$), and the interaction ($p = 0.0080$) were found for the fast component of inactivation (τ_1). Among the Kv4 isoforms, only Kv4.2 showed a significant Ca^{2+}-dependent acceleration of τ_1 (Kv4.1, $p = 0.9237$; Kv4.2, $p = 0.0004$; and Kv4.3, $p = 0.9373$). *f,* statistical tests showed no significant variation by treatment ($p = 0.9091$) or the interaction ($p = 0.5518$), whereas Kv4 isoform expression ($p = 0.0053$) affected the slow component of inactivation (τ_2). However, Ca^{2+} did not regulate τ_2 of any Kv4 isoform (Kv4.1, $p = 0.9088$; Kv4.2, $p = 0.9745$; and Kv4.3, $p = 0.7846$). *Error bars* represent mean ± S.E. *, $p < 0.05$; **, $p < 0.01$; ***, $p < 0.001$ by two-way ANOVA and Sidak's multiple comparison test. Refer to Table 1 for numerical data and replicate information.

voltage-activated K^+ channels (BK) has been put forward as an electrostatic switch that regulates palmitoylation state and plasma membrane channel density (49). The putative polybasic motif unique to KChIP2a1 and KChIP2a prevents Ca^{2+} regulation of Kv4 channels (Fig. 5*f*). More research will be required to determine whether alternative splicing of the putative polybasic motif in KChIP2 isoforms regulates Kv4 forward trafficking.

Ca^{2+} regulation of KChIP–Kv4 complexes in hippocampal dendrites

Ca^{2+} enhancement of Kv4 current density may function as a feedback mechanism to regulate excitability in tissues that express the appropriate KChIPs, including the heart and brain. *Kcnip1*, *Kcnip2*, *Kcnip3*, and *Kcnip4* gene transcripts have all been detected in the hippocampus. Although KChIP1 is primarily expressed in interneurons, KChIP2, KChIP3, and KChIP4 are abundantly expressed in excitatory neurons. However, the relative expression level of alternatively spliced KChIP transcripts in the hippocampus is still unknown. It is possible that hippocampal cell types have a specific complement of KChIP isoform expression providing varying levels or subcellular distribution of Kv4 channels in response to elevated intracellular Ca^{2+}. In the brain, alternative splicing is regulated in response to synaptic activity and mutations in mRNA splice sites can result in several pathophysiological diseases (50, 51). Therefore, splicing may act as a molecular switch to alter the KChIP complement to regulate Kv channel function. Putative Ca^{2+}-sensitive KChIPs in the hippocampus have been shown to respond to voltage-gated Ca^{2+} entry within a Kv4.2–Cav2.3 microdomain to regulate the size of excitatory postsynaptic potentials (52, 53). Further study is required to determine whether the Ca^{2+}-mediated changes in Kv4 channel density observed in this study regulate dendritic excitability and/or plasticity in hippocampal pyramidal neurons. Kv4.2 channels internalize to strengthen synaptic input in response to synaptic plasticity mechanisms (3). This process may be balanced by Ca^{2+} regulation of Kv4 surface expression during neuronal excitation, either through local ER release or influx through voltage-gated Ca^{2+} channels. Interestingly, Kv4 channels colocalize and are regulated by voltage-gated Ca^{2+} channels in the cerebellum (54) and hippocampus (53). Local Ca^{2+} concentrations within 50–100 nm of voltage-gated Ca^{2+} channels are theorized to exceed the 10 μM Ca^{2+} concentrations used in this study supporting the idea that local Ca^{2+} elevations in neurons could modulate Kv4 surface expression by the mechanism described in this report

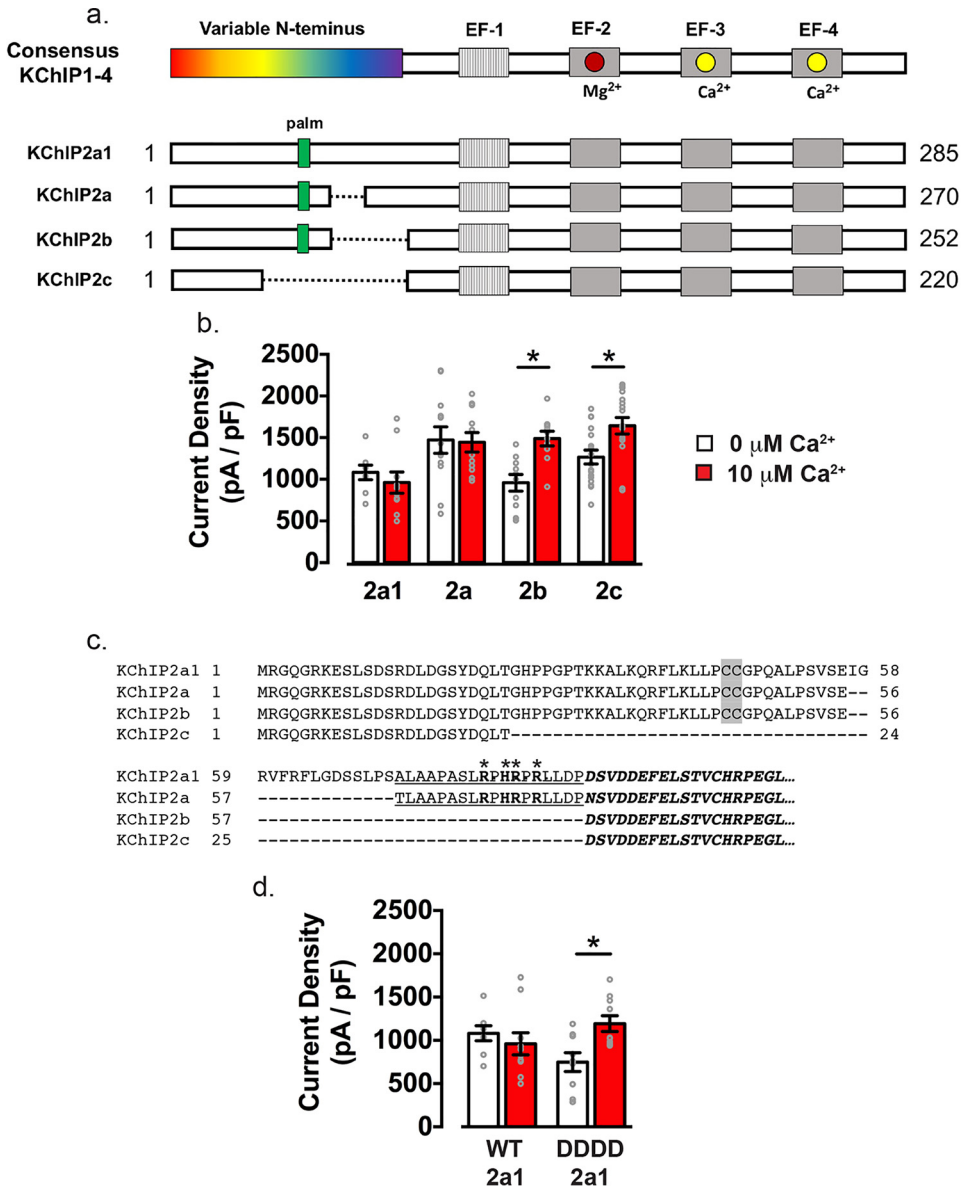

Figure 5. Ca^{2+} regulation of Kv4.2–KChIP2 complexes is KChIP isoform-dependent. *a,* consensus protein domain organization of KChIP family members (*top*). Protein domain organization of four KChIP2 isoforms that demonstrates N-terminal variability (*below*). *b,* two-way ANOVA returned significant differences in peak Kv4.2 current density between KChIP2 isoforms ($p = 0.0005$), by treatment ($p = 0.0227$), and the interaction ($p = 0.0150$). However, Kv4.2 peak current density was unaffected by intracellular Ca^{2+} when expressed with long forms of KChIP2 (KChIP2a1, $p = 0.9415$; KChIP2a, $p = 0.9997$), whereas Kv4.2 peak current was significantly increased in the presence of Ca^{2+} for shorter forms of KChIP2 (KChIP2b, $p = 0.0114$; KChIP2c, $p = 0.0203$). *c,* sequence alignment of human N-terminal domains of KChIP2 isoforms. The putative polybasic domain conserved in Ca^{2+}-insensitive KChIP isoforms is *underlined*, and basic residues are indicated with an *asterisk*. *d,* site-directed acidification of the putative polybasic motif in KChIP2a1 rescues Ca^{2+} enhancement of peak current density. Two-way ANOVA returned no differences between WT KChIP2a1 and mutant KChIP2a1 groups by construct expression ($p = 0.1419$) or treatment ($p = 0.6426$); however, the interaction was significant ($p = 0.0124$) likely due to differences in peak current density between WT and mutant KChIP2a1. Sidak's multiple comparison revealed that mutant KChIP2a1 responded to Ca^{2+} ($p = 0.0107$), whereas WT KChIP2a1 did not ($p = 0.6970$) as also shown in *b*. *Error bars,* mean ± S.E. *, $p < 0.05$; ***, $p < 0.001$ by two-way ANOVA and Sidak's multiple comparison test. Refer to Table 2 for numerical data and replicate information.

(55). Furthermore, Kv4 channels are known to regulate spike-timing–dependent plasticity by inhibiting back-propagation of action potentials (2). Further studies are needed to determine whether Ca^{2+}-KChIP–regulated enhancement of Kv4 current density in neuronal dendrites may affect spike-timing plasticity. In summary, we present a step forward in resolving an underlying mechanism for Ca^{2+} regulation of KChIP–Kv4 complexes. Ongoing efforts are aimed at understanding how Ca^{2+} regulation of KChIP–Kv4 function may mediate critical aspects of excitability and function of hippocampal dendrites.

Experimental procedures

Mammalian expression vectors

Heterologous Kv4 channel expression was carried out using human Kv4.1 (RC207353), Kv4.2 (RC215266), and Kv4.3 (RC219447) (Origene). Kv4 auxiliary subunit expression was carried out using human DPP6 (RC216919), human KChIP1a (RC224442), KChIP1b (RC208255), KChIP2a1 (RC213131), KChIP2b (RC203823), KChIP3a (RC203957), KChIP4bL (RC211488), KChIP4a (RC211613), and mouse KChIP2a

Table 3

Biophysical properties of Kv4.2–KChIP1, -3, and -4 isoform complexes in 0 μM free Ca^{2+} (gray) or ~10 μM free Ca^{2+} (red)

I_K indicates peak voltage-gated K^+ current. All entries describe the mean ± S.D.

Condition	$V_{1/2}$ VDA (mV)	$V_{1/2}$ VDI (mV)	Tau of RFI (ms)	I_K Density (pA/pF)	I_K 10-90% Rise (ms)	I_K Tau_1 (ms)	I_K Tau_2 (ms)
Kv4.2 only	-4.23 +/- 3.44 n = 18	-70.24 +/- 3.76 n = 17	125.3 +/- 25.65 n = 17	611.5 +/- 252.32 n = 20	2.53 +/- 0.72 n = 20	33.35 +/- 8.21 n = 20	139.3 +/- 28.26 n = 20
+ 10 μM Ca^{2+}	-7.39 +/- 4.34* n = 14	-71.05 +/- 6.96 n =12	111.6 +/- 20.33 n = 11	752.0 +/- 410.94 n = 18	1.89 +/- 0.51* n = 18	29.04 +/- 8.27 n = 18	126.6 +/- 33.35 n = 18
Kv4.2 KChIP1a	-10.24 +/- 1.59 n = 9	-68.82 +/- 1.59 n = 9	60.65 +/- 17.1 n = 9	515.8 +/- 250.3 n = 9	3.90 +/- 1.47 n = 9	59.91 +/- 15.27 n = 9	234.4 +/- 75.60 n = 9
+ 10 μM Ca^{2+}	-9.21 +/- 1.53 n = 8	-69.63 +/- 1.13 n = 8	59.68 +/- 13.78 n = 7	559.0 +/- 204.5 n = 8	3.13 +/- 0.82 n = 8	56.02 +/- 12.39 n = 8	193.7 +/- 20.00 n = 8
Kv4.2 KChIP1b	-20.81 +/- 2.02 n = 11	-69.38 +/- 1.63 n = 11	26.55 +/- 5.79 n = 10	952.7 +/- 377.4 n = 11	1.43 +/- 0.50 n = 11	93.03 +/- 38.14 n = 11	125.1 +/- 20.07 n = 11
+ 10 μM Ca^{2+}	-18.67 +/- 2.75 n = 11	-63.47 +/- 2.54* n = 7	19.06 +/- 8.36* n = 7	1143 +/- 492.4 n = 10	0.97 +/- 0.28* n = 10	86.16 +/- 35.32 n = 10	109.4 +/- 15.18 n = 10
Kv4.2 KChIP3a	-21.6 +/- 2.12 n = 16	-61.08 +/- 2.00 n = 16	14.64 +/- 3.52 n = 15	1073 +/- 342.0 n = 18	1.13 +/- 0.24 n = 18	126.9 +/- 28.02 n = 18	131.3 +/- 22.35 n = 18
+ 10 μM Ca^{2+}	-20.94 +/- 2.21 n = 15	-64.49 +/- 4.03* n = 15	15.03 +/- 2.81 n = 12	1470 +/- 371.7* n = 15	0.87 +/- 0.19* n = 15	112.5 +/- 22.28 n = 15	122.5 +/- 16.45 n = 15
Kv4.2 KChIP4bL	-10.77 +/- 1.66 n = 18	-54.00 +/- 1.59 n = 16	14.25 +/- 2.76 n = 14	1176 +/- 596.9 n = 16	1.48 +/- 0.45 n = 16	86.80 +/- 29.05 n = 16	115.7 +/- 28.82 n = 16
+ 10 μM Ca^{2+}	-9.61 +/- 1.85 n = 18	-55.99 +/- 1.75 n = 17	16.93 +/- 4.82 n = 13	1332 +/- 520.9 n = 14	1.42 +/- 0.39 n = 14	83.71+/- 48.47 n = 14	117.8 +/- 36.23 n = 14
Kv4.2 KChIP4a	-3.48 +/- 1.69 n = 13	-67.18 +/- 2.81 n = 13	96.49 +/- 34.22 n = 8	664.8 +/- 332.0 n = 10	3.612 +/- 0.82 n = 10	43.87 +/- 13.73 n = 10	283.8 +/- 99.90 n = 10
+ 10 μM Ca^{2+}	-2.35 +/- 1.67 n = 15	-68.09 +/- 3.05 n = 12	74.76 +/- 22.42 n = 10	773.6 +/- 230.6 n = 11	2.894 +/- 0.82 n = 11	38.78 +/- 10.22 n = 11	231.3 +/- 72.28 n = 11

* represents statistical significance ($0.05 > p > 0.0001$) by unpaired *t* test. All comparisons are made within each plasmid expression condition between 0 μM free Ca^{2+} and 10 μM free Ca^{2+}.

(MC211934) (Origene). Mouse KChIP2c was generously provided by Henry Jerng and Paul Pfaffinger (Baylor College of Medicine, Houston, TX). Site-directed mutagenesis to acidify hKChIP2a1 was outsourced to Bioinnovatise, LLC (Rockville, MD). Briefly, the plasmid sequence encoding SLRPH-RPRLL was acidified to SLDPDDPDLL by substitution of the WT sequence encoding the targeted basic amino acids of hKChIP2a1 (RC213131) to GAC aspartic acid codons.

Cell culture

HEK293T cells were maintained in Dulbecco's modified Eagle's medium (DMEM) supplemented with 10% fetal bovine serum and 2% penicillin/streptomycin (ThermoFisher Scientific) at 37 °C and 5% CO_2. Cells were passaged every 3–4 days at 80–95% confluency and reseeded at 800×10^6 cells in a 10-cm cell culture–treated Petri dish.

Heterologous channel expression

The day prior to transfection, cells were seeded onto 6-well cell culture–treated dishes at a concentration of 600×10^6 cells per well. After 16–20 h, plasmids encoding Kv4.2-WT (0.4 μg) and GFP (0.2 μg) were transfected using X-tremeGENE 9 (XG9; Sigma). Briefly, for each well, 5 μl of XG9 was added to 100 μl of minimum essential medium (MEM) and incubated

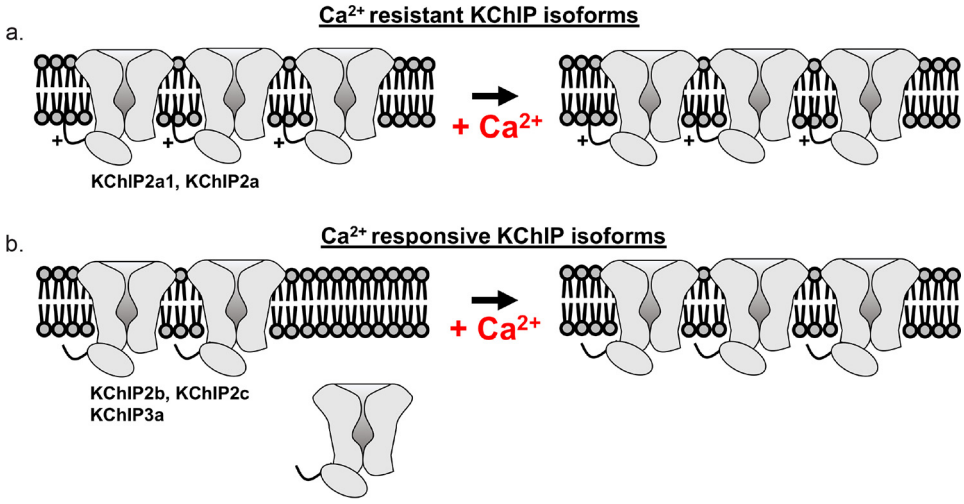

Figure 6. Model for Ca^{2+} regulation of Kv4–KChIP complexes. *a,* variable N-terminal domain of Ca^{2+}-resistant KChIP–Kv4 complexes share a conserved polybasic motif. *b,* Ca^{2+} regulates a subset of KChIP isoforms by promoting Kv4 channel current density.

≥5 min at room temperature. In a separate tube, plasmid DNA was added to 100 μl of MEM. After DNAs were added to MEM, this solution was mixed with the XG9/MEM solution and incubated at room temperature for 20 min. After XG9–DNA complexes were formed, the mixture was added dropwise to one well of the 6-well dish. 24–48 h after transfection, on the day of recording, transfected cultures were trypsinized for 2 min, washed, pelleted by centrifuge, resuspended in 5–10 ml of DMEM, and seeded at low density onto glass coverslips and allowed to adhere ≥1 h before recordings were started. Human Kv4.1 (0.5 μg), Kv4.2 (0.2 μg), and Kv4.3 (0.2 μg) were transfected with a molar excess of KChIP plasmid (1.0 μg of KChip, 0.5 μg of Kv4.1; 0.8 μg of KChIP, and 0.2 μg of Kv4.2/4.3) to ensure a 1:1 stoichiometry of Kv4/KChIP at the plasma membrane.

Electrophysiology

Coverslips were transferred to a recording chamber at room temperature and superfused (2–3 ml min^{-1}) in 95% O_2, 5% CO_2-saturated extracellular solution (in mM: 115 NaCl, 2.5 KCl, 1.25 NaH_2PO_4, 25 $NaHCO_3$, 2 $CaCl_2$, 1 $MgCl_2$, 25 glucose, pH 7.2–7.3, 300 mosM/liter) at 22–24 °C. The patch electrodes contained (in mM): 115 KCl, 10 NaCl, 20 KOH, 10 HEPES, and either 10 EGTA or 10 HEDTA and 5 $CaCl_2$. Patch-electrode solutions were brought up to pH 7.3–7.4 with KOH and adjusted to 290–300 mosM/liter using glucose. Peak currents were elicited by voltage steps from a holding potential of −60 to −120 mV for 400 ms to relieve channel inactivation and to +60 mV for 400 ms to achieve maximal channel activation. Inactivation rates were measured by fitting the falling phase of currents with a double-exponential decay (Fig. S1). Voltage dependence of activation was performed using the same holding and hyperpolarizing steps as above but with a range of intermediate activation potentials (−100, −80, −60, −40, −30, −20, and −10 and 0, +10, +20, +30, +40, and +60 mV). Conductance was calculated using the equation: $G = I_K/(V_m - V_{rev})$. Steady-state inactivation was performed using 400-ms conditioning steps from the holding potential to −140, −130, −120, −100, −80, −60, −40, −20, −10, and 0 mV immediately before a 400-ms step to the peak of current activation at +60 mV. Recovery from inactivation was measured using two 400-ms voltage steps to +60 mV from the holding potential separated by increasing time intervals (5, 10, 15, 20, 25, 50, 100, 200, and 500 ms). Electrophysiological recordings were obtained using a Multiclamp 700B amplifier and PClamp 10 (Molecular, Devices, Sunnyvale, CA). Currents were normalized to cell size using whole-cell capacitance upon cell break-in; liquid junction potential error was corrected on line (−6.5 mV in the pipette), and leak currents were subtracted using a P/4 protocol. Data were analyzed using Microsoft Excel, GraphPad Prism 6, and IGOR Pro (WaveMetrics, Lake Oswego, OR). When acquiring recordings for 0 Ca^{2+} and ~10 μM Ca^{2+} comparisons, all cells within a given genetic condition were performed on similar numbers of cells within the same day and also staggered by time of day. Pooled data are presented as either mean or box plots ± S.E. or S.D. where indicated.

Author contributions—J. G. M. and D. A. H. conceptualization; J. G. M. data curation; J. G. M. formal analysis; J. G. M. and D. A. H. funding acquisition; J. G. M. investigation; J. G. M. methodology; J. G. M. writing-original draft; J. G. M. and D. A. H. writing-review and editing; D. A. H. supervision.

Acknowledgments—We thank Manu Ben-Johny (Columbia University) and members of the Hoffman lab for advice and suggestions on this work.

References

1. Serôdio, P., Kentros, C., and Rudy, B. (1994) Identification of molecular components of A-type channels activating at subthreshold potentials. *J. Neurophysiol.* **72,** 1516–1529 CrossRef Medline
2. Hoffman, D. A., Magee, J. C., Colbert, C. M., and Johnston, D. (1997) K^+ channel regulation of signal propagation in dendrites of hippocampal pyramidal neurons. *Nature* **387,** 869–875 CrossRef Medline
3. Kim, J., Wei, D. S., and Hoffman, D. A. (2005) Kv4 potassium channel subunits control action potential repolarization and frequency-dependent broadening in rat hippocampal CA1 pyramidal neurones. *J. Physiol.* **569,** 41–57 CrossRef Medline
4. Ramakers, G. M., and Storm, J. F. (2002) A postsynaptic transient K^+ current modulated by arachidonic acid regulates synaptic integration and

threshold for LTP induction in hippocampal pyramidal cells. *Proc. Natl. Acad. Sci. U.S.A.* **99,** 10144–10149 CrossRef Medline
5. Chen, X., Yuan, L. L., Zhao, C., Birnbaum, S. G., Frick, A., Jung, W. E., Schwarz, T. L., Sweatt, J. D., and Johnston, D. (2006) Deletion of Kv4.2 gene eliminates dendritic A-type K^+ current and enhances induction of long-term potentiation in hippocampal CA1 pyramidal neurons. *J. Neurosci.* **26,** 12143–12151 CrossRef Medline
6. Lockridge, A., and Yuan, L. L. (2011) Spatial learning deficits in mice lacking A-type K^+ channel subunits. *Hippocampus* **21,** 1152–1156 CrossRef Medline
7. Johnston, D., Christie, B. R., Frick, A., Gray, R., Hoffman, D. A., Schexnayder, L. K., Watanabe, S., and Yuan, L. L. (2003) Active dendrites, potassium channels and synaptic plasticity. *Philos. Trans. R. Soc. Lond. B Biol. Sci.* **358,** 667–674 CrossRef Medline
8. Barnwell, L. F., Lugo, J. N., Lee, W. L., Willis, S. E., Gertz, S. J., Hrachovy, R. A., and Anderson, A. E. (2009) Kv4.2 knockout mice demonstrate increased susceptibility to convulsant stimulation. *Epilepsia* **50,** 1741–1751 CrossRef Medline
9. Bernard, C., Anderson, A., Becker, A., Poolos, N. P., Beck, H., and Johnston, D. (2004) Acquired dendritic channelopathy in temporal lobe epilepsy. *Science* **305,** 532–535 CrossRef Medline
10. Jerng, H. H., Kunjilwar, K., and Pfaffinger, P. J. (2005) Multiprotein assembly of Kv4.2, KChIP3 and DPP10 produces ternary channel complexes with ISA-like properties. *J. Physiol.* **568,** 767–788 CrossRef Medline
11. Nadal, M. S., Ozaita, A., Amarillo, Y., Vega-Saenz de Miera, E., Ma, Y., Mo, W., Goldberg, E. M., Misumi, Y., Ikehara, Y., Neubert, T. A., and Rudy, B. (2003) The CD26-related dipeptidyl aminopeptidase-like protein DPPX is a critical component of neuronal A-type K^+ channels. *Neuron* **37,** 449–461 CrossRef Medline
12. Rhodes, K. J., Carroll, K. I., Sung, M. A., Doliveira, L. C., Monaghan, M. M., Burke, S. L., Strassle, B. W., Buchwalder, L., Menegola, M., Cao, J., An, W. F., and Trimmer, J. S. (2004) KChIPs and Kv4 α subunits as integral components of A-type potassium channels in mammalian brain. *J. Neurosci.* **24,** 7903–7915 CrossRef Medline
13. An, W. F., Bowlby, M. R., Betty, M., Cao, J., Ling, H. P., Mendoza, G., Hinson, J. W., Mattsson, K. I., Strassle, B. W., Trimmer, J. S., and Rhodes, K. J. (2000) Modulation of A-type potassium channels by a family of calcium sensors. *Nature* **403,** 553–556 CrossRef Medline
14. Pruunsild, P., and Timmusk, T. (2005) Structure, alternative splicing, and expression of the human and mouse KCNIP gene family. *Genomics* **86,** 581–593 CrossRef Medline
15. Jerng, H. H., and Pfaffinger, P. J. (2014) Modulatory mechanisms and multiple functions of somatodendritic A-type K^+ channel auxiliary subunits. *Front. Cell. Neurosci.* **8,** 82 Medline
16. Shibata, R., Misonou, H., Campomanes, C. R., Anderson, A. E., Schrader, L. A., Doliveira, L. C., Carroll, K. I., Sweatt, J. D., Rhodes, K. J., and Trimmer, J. S. (2003) A fundamental role for KChIPs in determining the molecular properties and trafficking of Kv4.2 potassium channels. *J. Biol. Chem.* **278,** 36445–36454 CrossRef Medline
17. Kunjilwar, K., Qian, Y., and Pfaffinger, P. J. (2013) Functional stoichiometry underlying KChIP regulation of Kv4.2 functional expression. *J. Neurochem.* **126,** 462–472 CrossRef Medline
18. Chen, C. P., Lee, L., and Chang, L. S. (2006) Effects of metal-binding properties of human Kv channel-interacting proteins on their molecular structure and binding with Kv4.2 channel. *Protein J.* **25,** 345–351 CrossRef Medline
19. Lee, L., Chen, K. C., and Chang, L. S. (2009) Functional roles of EF-hands in human potassium channel-interacting protein 2.2. *Protein Pept. Lett.* **16,** 1081–1087 CrossRef Medline
20. Lin, Y. L., Chen, C. Y., Cheng, C. P., and Chang, L. S. (2004) Protein–protein interactions of KChIP proteins and Kv4.2. *Biochem. Biophys. Res. Commun.* **321,** 606–610 CrossRef Medline
21. Osawa, M., Dace, A., Tong, K. I., Valiveti, A., Ikura, M., and Ames, J. B. (2005) Mg^{2+} and Ca^{2+} differentially regulate DNA binding and dimerization of DREAM. *J. Biol. Chem.* **280,** 18008–18014 CrossRef Medline
22. Craig, T. A., Benson, L. M., Venyaminov, S. Y., Klimtchuk, E. S., Bajzer, Z., Prendergast, F. G., Naylor, S., and Kumar, R. (2002) The metal-binding properties of DREAM: evidence for calcium-mediated changes in DREAM structure. *J. Biol. Chem.* **277,** 10955–10966 CrossRef Medline
23. Pioletti, M., Findeisen, F., Hura, G. L., and Minor, D. L., Jr. (2006) Three-dimensional structure of the KChIP1–Kv4.3 T1 complex reveals a cross-shaped octamer. *Nat. Struct. Mol. Biol.* **13,** 987–995 CrossRef Medline
24. Bähring, R. (2018) Kv channel-interacting proteins as neuronal and non-neuronal calcium sensors. *Channels* **12,** 187–200 CrossRef Medline
25. Bähring, R., Dannenberg, J., Peters, H. C., Leicher, T., Pongs, O., and Isbrandt, D. (2001) Conserved Kv4 N-terminal domain critical for effects of Kv channel-interacting protein 2.2 on channel expression and gating. *J. Biol. Chem.* **276,** 23888–23894 CrossRef Medline
26. Morohashi, Y., Hatano, N., Ohya, S., Takikawa, R., Watabiki, T., Takasugi, N., Imaizumi, Y., Tomita, T., and Iwatsubo, T. (2002) Molecular cloning and characterization of CALP/KChIP4, a novel EF-hand protein interacting with presenilin 2 and voltage-gated potassium channel subunit Kv4. *J. Biol. Chem.* **277,** 14965–14975 CrossRef Medline
27. Gonzalez, W. G., Pham, K., and Miksovska, J. (2014) Modulation of the voltage-gated potassium channel (Kv4.3) and the auxiliary protein (KChIP3) interactions by the current activator NS5806. *J. Biol. Chem.* **289,** 32201–32213 CrossRef Medline
28. Takimoto, K., Yang, E. K., and Conforti, L. (2002) Palmitoylation of KChIP splicing variants is required for efficient cell surface expression of Kv4.3 channels. *J. Biol. Chem.* **277,** 26904–26911 CrossRef Medline
29. Ben-Johny, M., Yang, P. S., Niu, J., Yang, W., Joshi-Mukherjee, R., and Yue, D. T. (2014) Conservation of Ca^{2+}/calmodulin regulation across Na and Ca^{2+} channels. *Cell* **157,** 1657–1670 CrossRef Medline
30. Cembrowski, M. S., Wang, L., Sugino, K., Shields, B. C., and Spruston, N. (2016) Hipposeq: a comprehensive RNA-seq database of gene expression in hippocampal principal neurons. *Elife* **5,** e14997 CrossRef Medline
31. Lein, E. S., Hawrylycz, M. J., Ao, N., Ayres, M., Bensinger, A., Bernard, A., Boe, A. F., Boguski, M. S., Brockway, K. S., Byrnes, E. J., Chen, L., Chen, L., Chen, T. M., Chin, M. C., Chong, J., *et al.* (2007) Genome-wide atlas of gene expression in the adult mouse brain. *Nature* **445,** 168–176 CrossRef Medline
32. Serôdio, P., and Rudy, B. (1998) Differential expression of Kv4 K^+ channel subunits mediating subthreshold transient K^+ (A-type) currents in rat brain. *J. Neurophysiol.* **79,** 1081–1091 CrossRef Medline
33. Marionneau, C., LeDuc, R. D., Rohrs, H. W., Link, A. J., Townsend, R. R., and Nerbonne, J. M. (2009) Proteomic analyses of native brain K(V)4.2 channel complexes. *Channels* **3,** 284–294 Medline
34. Chang, L. S., Chen, C. Y., and Wu, T. T. (2003) Functional implication with the metal-binding properties of KChIP1. *Biochem. Biophys. Res. Commun.* **311,** 258–263 CrossRef Medline
35. Piazza, M., Taiakina, V., Dieckmann, T., and Guillemette, J. G. (2017) Structural consequences of calmodulin EF hand mutations. *Biochemistry* **56,** 944–956 CrossRef Medline
36. Groen, C., and Bähring, R. (2017) Modulation of human Kv4.3/KChIP2 channel inactivation kinetics by cytoplasmic Ca^{2+}. *Pflugers Arch.* **469,** 1457–1470 CrossRef Medline
37. Hasdemir, B., Fitzgerald, D. J., Prior, I. A., Tepikin, A. V., and Burgoyne, R. D. (2005) Traffic of Kv4 K^+ channels mediated by KChIP1 is via a novel post-ER vesicular pathway. *J. Cell Biol.* **171,** 459–469 CrossRef Medline
38. Foeger, N. C., Marionneau, C., and Nerbonne, J. M. (2010) Co-assembly of Kv4 α subunits with K^+ channel-interacting protein 2 stabilizes protein expression and promotes surface retention of channel complexes. *J. Biol. Chem.* **285,** 33413–33422 CrossRef Medline
39. Beck, E. J., Bowlby, M., An, W. F., Rhodes, K. J., and Covarrubias, M. (2002) Remodelling inactivation gating of Kv4 channels by KChIP1, a small-molecular-weight calcium-binding protein. *J. Physiol.* **538,** 691–706 CrossRef Medline
40. Lusin, J. D., Vanarotti, M., Li, C., Valiveti, A., and Ames, J. B. (2008) NMR structure of DREAM: implications for Ca^{2+}-dependent DNA binding and protein dimerization. *Biochemistry* **47,** 2252–2264 CrossRef Medline
41. Scannevin, R. H., Wang, K., Jow, F., Megules, J., Kopsco, D. C., Edris, W., Carroll, K. C., Lü, Q., Xu, W., Xu, Z., Katz, A. H., Olland, S., Lin, L., Taylor, M., Stahl, M., *et al.* (2004) Two N-terminal domains of Kv4 K^+ channels regulate binding to and modulation by KChIP1. *Neuron* **41,** 587–598 CrossRef Medline

42. Liang, P., Wang, H., Chen, H., Cui, Y., Gu, L., Chai, J., and Wang, K. (2009) Structural Insights into KChIP4a modulation of Kv4.3 inactivation. *J. Biol. Chem.* **284,** 4960–4967 CrossRef Medline
43. Wang, H., Yan, Y., Liu, Q., Huang, Y., Shen, Y., Chen, L., Chen, Y., Yang, Q., Hao, Q., Wang, K., and Chai, J. (2007) Structural basis for modulation of Kv4 K^+ channels by auxiliary KChIP subunits. *Nat. Neurosci.* **10,** 32–39 CrossRef Medline
44. Gebauer, M., Isbrandt, D., Sauter, K., Callsen, B., Nolting, A., Pongs, O., and Bähring, R. (2004) N-type inactivation features of Kv4.2 channel gating. *Biophys. J.* **86,** 210–223 CrossRef Medline
45. Jerng, H. H., and Pfaffinger, P. J. (2008) Multiple Kv channel-interacting proteins contain an N-terminal transmembrane domain that regulates Kv4 channel trafficking and gating. *J. Biol. Chem.* **283,** 36046–36059 CrossRef Medline
46. Ramachandran, P. L., Craig, T. A., Atanasova, E. A., Cui, G., Owen, B. A., Bergen, H. R., 3rd, Mer, G., and Kumar, R. (2012) The potassium channel interacting protein 3 (DREAM/KChIP3) heterodimerizes with and regulates calmodulin function. *J. Biol. Chem.* **287,** 39439–39448 CrossRef Medline
47. Lin, L., Sun, W., Kung, F., Dell'Acqua, M. L., and Hoffman, D. A. (2011) AKAP79/150 impacts intrinsic excitability of hippocampal neurons through phospho-regulation of A-type K^+ channel trafficking. *J. Neurosci.* **31,** 1323–1332 CrossRef Medline
48. Yao, J. J., Zhao, Q. R., Liu, D. D., Chow, C. W., and Mei, Y. A. (2016) Neuritin up-regulates Kv4.2 α-subunit of potassium channel expression and affects neuronal excitability by regulating the calcium-calcineurin-NFATc4 signaling pathway. *J. Biol. Chem.* **291,** 17369–17381 CrossRef Medline
49. Jeffries, O., Tian, L., McClafferty, H., and Shipston, M. J. (2012) An electrostatic switch controls palmitoylation of the large conductance voltage- and calcium-activated potassium (BK) channel. *J. Biol. Chem.* **287,** 1468–1477 CrossRef Medline
50. Licatalosi, D. D., and Darnell, R. B. (2006) Splicing regulation in neurologic disease. *Neuron* **52,** 93–101 CrossRef Medline
51. Lipscombe, D. (2005) Neuronal proteins custom designed by alternative splicing. *Curr. Opin. Neurobiol.* **15,** 358–363 CrossRef Medline
52. Wang, K., Kelley, M. H., Wu, W. W., Adelman, J. P., and Maylie, J. (2015) Apamin boosting of synaptic potentials in CaV2.3 R-Type Ca^{2+} channel null mice. *PLoS ONE* **10,** e0139332 CrossRef Medline
53. Wang, K., Lin, M. T., Adelman, J. P., and Maylie, J. (2014) Distinct Ca^{2+} sources in dendritic spines of hippocampal CA1 neurons couple to SK and Kv4 channels. *Neuron* **81,** 379–387 CrossRef Medline
54. Anderson, D., Mehaffey, W. H., Iftinca, M., Rehak, R., Engbers, J. D., Hameed, S., Zamponi, G. W., and Turner, R. W. (2010) Regulation of neuronal activity by Cav3–Kv4 channel signaling complexes. *Nat. Neurosci.* **13,** 333–337 CrossRef Medline
55. Matthews, E. A., and Dietrich, D. (2015) Buffer mobility and the regulation of neuronal calcium domains. *Front. Cell Neurosci.* **9,** 48 Medline